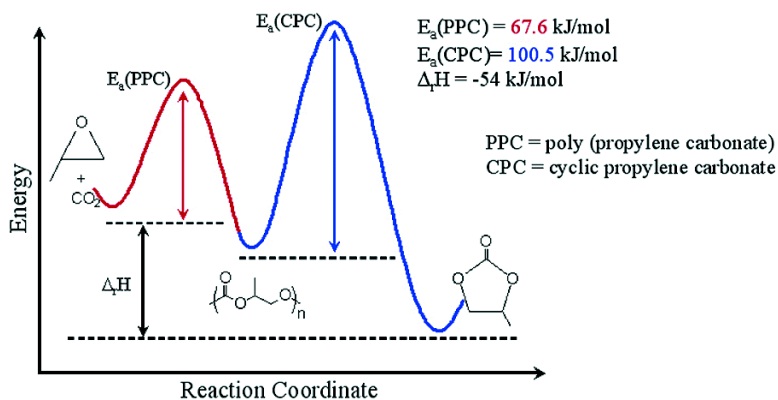


## Comparative Kinetic Studies of the Copolymerization of Cyclohexene Oxide and Propylene Oxide with Carbon Dioxide in the Presence of Chromium Salen Derivatives. In Situ FTIR Measurements of Copolymer vs Cyclic Carbonate Production

Donald J. Darensbourg, Jason C. Yarbrough, Cesar Ortiz, and Cindy C. Fang

*J. Am. Chem. Soc.*, **2003**, 125 (25), 7586-7591 • DOI: 10.1021/ja034863e • Publication Date (Web): 03 June 2003

Downloaded from <http://pubs.acs.org> on March 29, 2009



### More About This Article

Additional resources and features associated with this article are available within the HTML version:

- Supporting Information
- Links to the 16 articles that cite this article, as of the time of this article download
- Access to high resolution figures
- Links to articles and content related to this article
- Copyright permission to reproduce figures and/or text from this article

[View the Full Text HTML](#)

## Comparative Kinetic Studies of the Copolymerization of Cyclohexene Oxide and Propylene Oxide with Carbon Dioxide in the Presence of Chromium Salen Derivatives. In Situ FTIR Measurements of Copolymer vs Cyclic Carbonate Production

Donald. J. Darensbourg,\* Jason C. Yarbrough, Cesar Ortiz, and Cindy C. Fang

Contribution from the Department of Chemistry, Texas A&M University,  
College Station, Texas 77843

Received February 25, 2003; E-mail: djdarens@mail.chem.tamu.edu.

**Abstract:** The catalysis of the reaction of carbon dioxide with epoxides (cyclohexene oxide or propylene oxide) using the (salen)Cr<sup>III</sup>Cl complex as catalyst, where H<sub>2</sub>salen = *N,N*-bis(3,5-di-*tert*-butylsalicylidene)-1,2-cyclohexenediimine (**1**), to provide copolymer and cyclic carbonate has been investigated by in situ infrared spectroscopy. As previously demonstrated for the cyclohexene oxide/CO<sub>2</sub> reaction in the presence of complex **1**, coupling of propylene oxide and carbon dioxide was found to occur by way of a pathway first-order in catalyst concentration. Unlike the cyclohexene oxide/carbon dioxide reaction catalyzed by complex **1**, which affords completely alternating copolymer and only small quantities of trans-cyclic cyclohexyl carbonate, under similar conditions propylene oxide/carbon dioxide produces mostly cyclic propylene carbonate. Comparative kinetic measurements were performed as a function of reaction temperature to assess the activation barrier for production of cyclic carbonates and polycarbonates for the two different classes of epoxides, i.e., alicyclic (cyclohexene oxide) and aliphatic (propylene oxide). As anticipated in both instances the unimolecular pathway for cyclic carbonate formation has a larger energy of activation than the bimolecular enchainment pathway. That is, the energies of activation determined for cyclic propylene carbonate and poly(propylene carbonate) formation were 100.5 and 67.6 kJ·mol<sup>-1</sup>, respectively, compared to the corresponding values for cyclic cyclohexyl carbonate and poly(cyclohexylene carbonate) production of 133 and 46.9 kJ·mol<sup>-1</sup>. The small energy difference in the two concurrent reactions for the propylene oxide/CO<sub>2</sub> process (33 kJ·mol<sup>-1</sup>) accounts for the large quantity of cyclic carbonate produced at elevated temperatures in this instance.

### Introduction

Few synthetic processes have been developed incorporating the ubiquitous small molecule, *carbon dioxide*, as a C<sub>1</sub> starting material.<sup>1</sup> Nevertheless, interest in developing effective methods for harnessing such a substantial and underutilized source of carbon is significant. This is especially true for the production of materials or intermediates which have a large worldwide production annually. Indeed, a topic of much current research activity has been the development of well-defined transition metal complexes as homogeneous catalysts or catalyst precursors for the copolymerization of CO<sub>2</sub> and epoxides to produce poly(cyclohexylene carbonate).<sup>2</sup> From an economic point of view this process holds obvious advantages, especially in instances where the epoxides are derived from renewable resources, e.g.,  $\alpha$ -pinene oxide or limonene oxide. In addition within the context of the current production of polycarbonates, which is highly

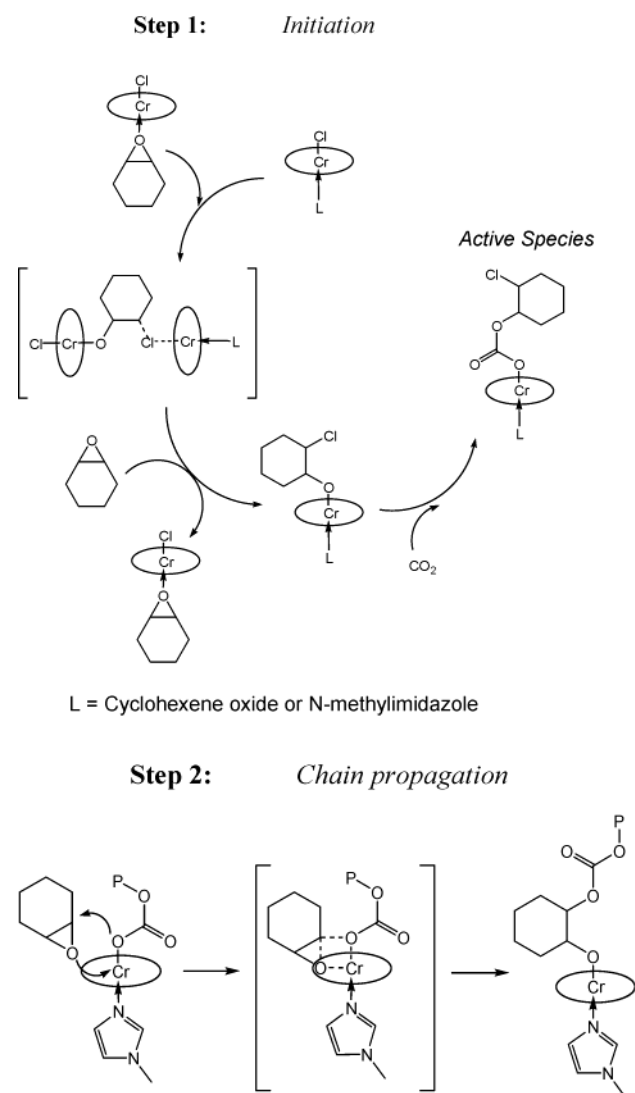
dependent on the use of phosgene or its derivatives, the elaboration of commercially viable alternatives for production of selected polycarbonates is highly attractive from an environmental standpoint. Presently, the industrially important polycarbonate is synthesized from 2,2-bis(4-hydroxyphenyl)propane (bisphenolA) and diphenyl carbonate. The plausibility of the copolymerization of CO<sub>2</sub> and epoxides was first demonstrated by Inoue and co-workers in 1969, where it was shown that a heterogeneous catalyst derived from diethyl zinc and water was active for this process.<sup>3</sup> This route to polycarbonates was subsequently made more feasible with the uncovering of more

(1) (a) Gibson, D. H. *Chem. Rev.* **1996**, *96*, 2063–2095. (b) Leitner, W. *Coord. Chem. Rev.* **1996**, *155*, 257–284. (c) Yin, X.; Moss, J. R. *Coord. Chem. Rev.* **1999**, *181*, 27–59. (d) Aresta, M.; Schloss, J. V., Eds. *Enzymatic and Model Carboxylation and Reduction Reactions for Carbon Monoxide Utilization*; NATO ASI Series, C314; Kluwer: Dordrecht, The Netherlands, 1990. (e) Brauden, C.-I., Schneider, G., Eds. *Carbon Dioxide Fixation and Reduction in Biological and Model Systems*; Oxford University Press: Oxford, U.K., 1994.

(2) (a) Darensbourg, D. J.; Holtcamp, M. W. *Macromolecules* **1995**, *28*, 7577–7579. (b) Super, M.; Berluche, E.; Costello, C.; Beckman, E. *Macromolecules* **1997**, *30*, 368–372. (c) Super, M.; Beckman, E. *J. Macromol. Symp.* **1998**, *127*, 89–108. (d) Cheng, M.; Lobkovsky, E. B.; Coates, G. W. *J. Am. Chem. Soc.* **1998**, *120*, 11018–11019. (e) Beckman, E. *Science* **1999**, *283*, 946–947. (f) Darensbourg, D. J.; Holtcamp, M. W.; Struck, G. E.; Zimmer, M. S.; Niezgodna, S. A.; Rainey, P.; Robertson, J. B.; Draper, J. D.; Reibenspies, J. H. *J. Am. Chem. Soc.* **1999**, *121*, 107–116. (g) Darensbourg, D. J.; Wildeson, J. R.; Yarbrough, J. C.; Reibenspies, J. H. *J. Am. Chem. Soc.* **2000**, *122*, 12487–12496. (h) Cheng, M.; Moore, D. R.; Reczek, J. J.; Chamberlain, B. M.; Lobkovsky, B. E.; Coates, G. W. *J. Am. Chem. Soc.* **2001**, *123*, 8738–8749. (i) Cheng, M.; Darling, N. A.; Lobkovsky, E. B.; Coates, G. W. *Chem. Commun.* **2000**, 2007–2008. (j) Eberhardt, R.; Allmendinger, M.; Luinstra, G. A.; Rieger, B. *Organometallics* **2003**, *22*, 211–214.

(3) Inoue, S.; Koinuma, H.; Tsuruta, T. *J. Polym. Sci., Part B: Polym. Lett.* **1969**, *7*, 287–292.

Scheme 1



active zinc catalysts derived from zinc oxide and dicarboxylic acids by Soga and co-workers.<sup>4</sup> These later catalysts (or catalyst precursors) are used in the commercial production of poly(propylene carbonate) and poly(ethylene carbonate).<sup>5</sup>

In a recent publication we presented an initial mechanistic study of the carbon dioxide/(cyclohexene oxide or propylene oxide) coupling process using (salen)CrCl (salen = *N,N'*-bis(3,5-di-*tert*-butylsalicylidene)-1,2-cyclohexanediiimine) as a catalyst.<sup>6</sup> Unlike the zinc catalysts previously investigated, this and other closely related systems<sup>7</sup> do not possess a site for epoxide binding in close proximity to a nucleophile for the rate-determining epoxide ring-opening step. However, this issue has been addressed by Jacobsen and co-workers in their studies of

asymmetric ring-opening of epoxides.<sup>8</sup> That is, these researchers found a second-order rate dependence on catalyst loading and proposed an asymmetric ring opening (ARO) mechanism proceeding via a dinuclear transition state (see step 1 of Scheme 1). On the other hand, our investigations showed there to be *no* stereocontrol associated with epoxide incorporation, as evidenced by the <sup>13</sup>C NMR spectra of the copolymers produced.<sup>6,9</sup> Consistent with the lack of stereocontrol, it was shown that in this instance there was a first-order dependence of the chain propagation step on the catalyst concentration. Additionally, it was discovered that, in the presence of various amounts of the neutral Lewis base cocatalyst, *N*-methylimidazole (*N*-MeIm), the rate of chain propagation was dramatically enhanced. These observations led to our proposal of a mechanistic pathway for copolymer production proceeding through a Jacobsen initiation step followed by chain propagation involving a concerted insertion of epoxide (Scheme 1).

Presently, we will communicate studies aimed at further assessing the credibility of the mechanistic interpretation of the CO<sub>2</sub>/epoxide coupling process depicted in Scheme 1. The investigation reported herein involves a much warranted temperature-dependent kinetic study of the relative propensity of these catalyst systems for producing copolymer vs cyclic carbonate as a function of the nature of the epoxide (propylene oxide and cyclohexene oxide).

## Experimental Section

### Reagents and Methods.

Methylene chloride, ethanol, diethyl ether, toluene, tetrahydrofuran (THF), and pentane were freshly distilled from the appropriate reagents immediately prior to use. *N,N'*-Bis(3,5-di-*tert*-butylsalicylidene)-1,2-cyclohexene diimine and 3,5-di-*tert*-butyl salicylaldehyde were purchased either from Aldrich Chemical Co. or Strem and used without further purification. *N*-(2,6-diisopropylphenyl)-3-phenyl salicylaldehyde, *N*-(2,6-diisopropylphenyl)salicylaldehyde,<sup>10</sup> and (salen)Cr<sup>III</sup>Cl (**1**) (salen = *N,N'*-bis(3,5-di-*tert*-butylsalicylidene)-1,2-cyclohexanediiimine) were prepared as described in the literature.<sup>8</sup> Unless otherwise specified, all manipulations were carried out on a double manifold Schlenk vacuum line under an atmosphere of argon or in an argon-filled glovebox. <sup>1</sup>H and <sup>13</sup>C NMR spectra were acquired on Unity+ 300 MHz and VXR 300 MHz superconducting NMR spectrometers. Infrared spectra were recorded on a Mattson 6021 FTIR spectrometer with DTGS and MCT detectors.

**Synthesis of Bis(3-*R*-salicylaldehyde) Chromium(III) Chloride Acetonitrile Complexes (2a,b) (2a, *R* = H; 2b, *R* = Ph).** The synthesis of these complexes has been reported elsewhere.<sup>10b</sup> However, modifications to those procedures compel us to report the details of our synthetic approach. To a 50-mL Schlenk flask containing the appropriate ligand (5.33 mmol), in 25 mL of Et<sub>2</sub>O, *n*-butyllithium (5.33 mmol) was added at -78 °C. The resulting yellow solution was allowed to stir for 2 h. The solution was then transferred to a flask containing CrCl<sub>3</sub>·3THF (2.0 g, 5.33 mmol) in 10 mL of THF, and the resulting green mixture was stirred overnight. After filtration to remove LiCl, the solvent was removed under vacuum, and 30 mL of acetonitrile was added. The green solution was stirred for 4 h and filtered and the solvent removed.

(4) Soga, K.; Imai, E.; Hattori, I. *Polym. J.* **1981**, *13*, 407–410.  
 (5) (a) Rokicki, A. (Air Products and Chemicals, Inc., and Acro Chemical Co.). U.S. Patent 4,943,677, 1990. (b) Motika, S. (Air Products and Chemicals, Inc., and Acro Chemical Co., and Mitsui Petrochemical Industries Ltd.). U.S. Patent 5,026,676, 1991. (c) Empower Materials, Newark, DE; a subsidiary of Axess Corp. of Greenville, Delaware.  
 (6) Darenbourg, D. J.; Yarbrough, J. C. *J. Am. Chem. Soc.* **2002**, *124*, 6335–6342.  
 (7) (a) Inoue, S. *J. Polym. Sci., Part A: Polym. Chem.* **2000**, *38*, 2861–2871. (b) Kruper, W. J.; Dellar, D. V. *J. Org. Chem.* **1995**, *60*, 725–727. (c) Mang, S.; Cooper, A. I.; Colclough, M. E.; Chauhan, N.; Holmes, A. B. *Macromolecules* **2000**, *33*, 303–308. (d) Paddock, R. L.; Nguyen, S. T. *J. Am. Chem. Soc.* **2001**, *123*, 11498–11499. (e) Eberhardt, R.; Allmendinger, M.; Rieger, B. *Macromol. Rapid Commun.* **2003**, *24*, 194–196.

(8) (a) Martinez, L. E.; Leighton, J. L.; Carsten, D. H.; Jacobsen, E. N. *J. Am. Chem. Soc.* **1995**, *117*, 5897–5898. (b) Hansen, K. B.; Leighton, J. L.; Jacobsen, E. N. *J. Am. Chem. Soc.* **1996**, *118*, 10924–10925. (c) Jacobsen, E. N. *Acc. Chem. Res.* **2000**, *33*, 421–431.  
 (9) (a) Nozaki, K.; Nakano, K.; Hiyama, T. *J. Am. Chem. Soc.* **1999**, *121*, 11008–11009. (b) Nakano, K.; Nozaki, K.; Hiyama, T. *Macromolecules* **2001**, *34*, 6325–6332. (c) See ref 2i.  
 (10) (a) Roland, S.; Mangeney, P. *Eur. J. Org. Chem.* **2000**, 611–616. (b) Gibson, V. C.; Mastroianni, S.; Newton, C.; Redshaw, C.; Solan, G. A.; White, A. J. P.; Williams, D. J. *J. Chem. Soc., Dalton Trans.* **2000**, 1969–1971.

**Table 1.** Crystallographic Data and Data Collection Parameters for **2b**

|                   |  |  |           |
|-------------------|--|--|-----------|
| empirical formula | C <sub>68</sub> H <sub>76</sub> N <sub>3</sub> O <sub>2</sub> ClCr | V, Å <sup>3</sup>                      | 10 577(4) |
| FW                | 1054.77  | Z                                      | 8         |
| cryst syst        | monoclinic   | T, K                                   | 110(2)    |
| space group       | P2 <sub>1</sub> /n   | D <sub>calc</sub> d, Mg/m <sup>3</sup> | 1.325     |
| a, Å              | 22.370(5)  | absorp coeff, mm <sup>-1</sup>         | 0.319     |
| b, Å              | 20.764(5)  | GOF                                    | 0.661     |
| c, Å              | 23.028(6)  | R, % [I > 2σ(I)]                       | 7.91      |
| β, deg            | 98.579(5)  | R <sub>w</sub> , % [I > 2σ(I)]         | 17.63     |

$$^a R = \sum ||F_o| - |F_c|| / \sum F_o, R_w = \{[(F_o^2 - F_c^2)^2] / [\sum (F_o^2)^2]\}^{1/2}.$$

**X-ray Structural Study (2b).** Suitable crystals for X-ray analysis were obtained by slow diffusion of pentane into a toluene solution of **2b**. Crystal data and details on collection parameters are given in Table 1. The X-ray data were collected on a Bruker Smart 1000 CCD diffractometer and covered more than a hemisphere of reciprocal space by a combination of three sets of exposures; each exposure set had a different  $\varphi$  angle for the crystal orientation and each exposure covered 0.3° in  $\omega$ . The crystal to detector distance was 4.9 cm. Decay was monitored by repeating collection of the 50 initial frames collected and analyzing the duplicate reflections. Crystal decay was negligible in both cases. The space group was determined on the basis of systematic absences and intensity statistics.<sup>11</sup> The structures were solved by direct methods and refined by full-matrix least squares on  $F^2$ . All non-hydrogen atoms were refined with anisotropic displacement parameters. All H atoms were placed at idealized positions and refined with fixed isotropic displacement parameters equal to 1.2 (1.5 for methyl protons) times the equivalent isotropic displacement parameters of the atoms—to which they were attached.

The following are the programs that were used: data collection and cell refinement, SMART;<sup>11</sup> data reduction, SAINTPLUS (Bruker<sup>12</sup>); programs used to solve structures, SHELXS-86 (Sheldrick<sup>13</sup>); programs used to refine structures, SHELXL-97 (Sheldrick<sup>14</sup>); molecular graphics and preparation of material for publication, SHELXTL-Plus version 5.0 (Bruker<sup>15</sup>).

#### Copolymerization Reactions of Epoxides and CO<sub>2</sub>.

A typical polymerization experiment was carried out as follows: Approximately 50 mg of complex **1** or **2b** was dissolved in 20 mL of the appropriate epoxide. The solution was then loaded via injection port into a 300-mL autoclave, which had been previously dried under vacuum overnight at 80 °C. The autoclave was placed under 48.3 bar in CO<sub>2</sub> and heated to 80 °C (approximately 60 bar at reaction temperature). The reaction was allowed to stir for 24 h at which time stirring was discontinued and the autoclave allowed to return to room temperature. The polymer was extracted as a methylene chloride solution and subjected to repeated precipitation with methanol.

The collected polycarbonate copolymers were analyzed by <sup>1</sup>H NMR, where protons adjacent to carbonate linkages afford a signal at 4.6 ppm while the absence of polyether linkages was verified by the absence of a signal at 3.5 ppm. Further, infrared spectra were collected to verify the presence of the  $\nu(\text{CO}_2)$  stretch at 1750 cm<sup>-1</sup> due to polycarbonate. To determine polymer tacticity, <sup>13</sup>C NMR spectroscopy was employed and analyzed as described recently by Nozaki and co-workers.<sup>9b</sup> Chemical shifts observed at 153.8, 153.4, and 153.2 ppm indicate the production of largely atactic polymer.

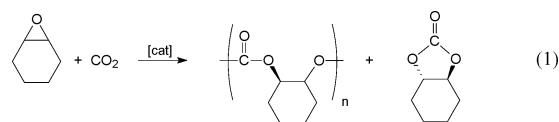
#### Copolymerization Reactions Monitored by IR Spectroscopy.

In a typical experiment, 10 mL of neat cyclohexene oxide was delivered via the injection port into a 300-mL stainless steel Parr autoclave reactor. The reactor is modified with a silicon window to allow for the use of

an ASI ReactIR 1000 system equipped with a MCT detector and 30 bounce SiCOMP in situ probe. In this manner, a single 128-scan background spectrum was collected. The catalyst (in 30 mL of neat cyclohexene oxide) was then injected into the reactor via the injection port, resulting in a 40-mL reaction solution. The reactor was pressurized to 48.3 bar in CO<sub>2</sub> and heated to the desired temperature as the IR probe began collecting scans. The infrared spectrometer was set up to collect one spectrum every 3 min over an 18-hour period. Profiles of the absorbance at 1750 cm<sup>-1</sup>( $\nu(\text{CO}_2)$ ) for the carbonate functionality with time were recorded and used to provide initial reaction rates for analysis. (Note: Catalyst loading varied with the experiment as described in Results and Discussion.)

## Results and Discussion

Previously, we have reported kinetic data for the reaction defined in eq 1, employing complex **1** as catalyst, obtained by monitoring the progress of the reaction by in situ infrared spectroscopy.<sup>6</sup> Both the substrate enchainment steps and cyclic carbonate formation were shown to exhibit a first-order dependence on the catalyst concentration. Herein, we have extended these investigations to include the epoxide, propylene oxide, which has a strong propensity for producing cyclic carbonate instead of polycarbonate.



A series of carbon dioxide/propylene oxide coupling reactions were performed as a function of catalyst (complex **1**) loading, while the formation of copolymer and cyclic carbonate was simultaneously monitored by in situ infrared spectroscopy. The reactions were carried out in a 300-mL Parr autoclave reactor, modified to accommodate an ASI ReactIR SiCOMP probe, in 40 mL of a toluene/propylene oxide (4:1) solvent mixture at 40 °C under 750 psi of carbon dioxide. Figure 1 illustrates a typical profile of the infrared absorbance at 1752 cm<sup>-1</sup> due to poly(propylene carbonate) production with time. Under these reaction conditions only a small amount of the cyclic carbonate (propylene carbonate) is produced, as seen by the infrared band at 1802 cm<sup>-1</sup>. As noted in our initial report, there is a time period required to activate the catalyst. This activation time is highly dependent, both on the nature of the catalyst and on its concentration. These observations are consistent with our assertion that the catalysis first proceeds through an activation (ARO) step, as described by Jacobsen in Scheme 1 (step 1).<sup>8</sup> Therefore, to obtain rate data for the enchainment steps, we analyzed data from the linear region of the reaction profiles, the slope of which is proportional to the rate of chain propagation. As seen in Figure 2, these rates exhibit linear behavior vs [catalyst]. These findings are entirely analogous to the earlier results obtained for cyclohexene oxide as a substrate for a process carried out at higher temperature (80 °C) and are in compliance with our mechanistic proposal (Scheme 1 (step 2)).

In contrast to the cyclohexene oxide/carbon dioxide copolymerization reaction when the propylene oxide/carbon dioxide process is performed at elevated temperatures (e.g., 80 °C), propylene carbonate is the dominant product. It has been proposed, and generally accepted, that production of cyclic carbonates during the copolymerization reaction is the result

- (11) SMART 1000 CCD; Bruker Analytical X-ray Systems: Madison, WI, 1999.  
 (12) SAINT-Plus, version 6.02; Bruker: Madison, WI, 1999.  
 (13) Sheldrick, G. SHELXS-86: Program for Crystal Structure Solution; Institut für Anorganische Chemie der Universität: Göttingen, Germany, 1986.  
 (14) Sheldrick, G. SHELXL-97: Program for Crystal Structure Refinement; Institut für Anorganische Chemie der Universität: Göttingen, Germany, 1997.  
 (15) SHELXTL, version 5.0; Bruker: Madison, WI, 1999.



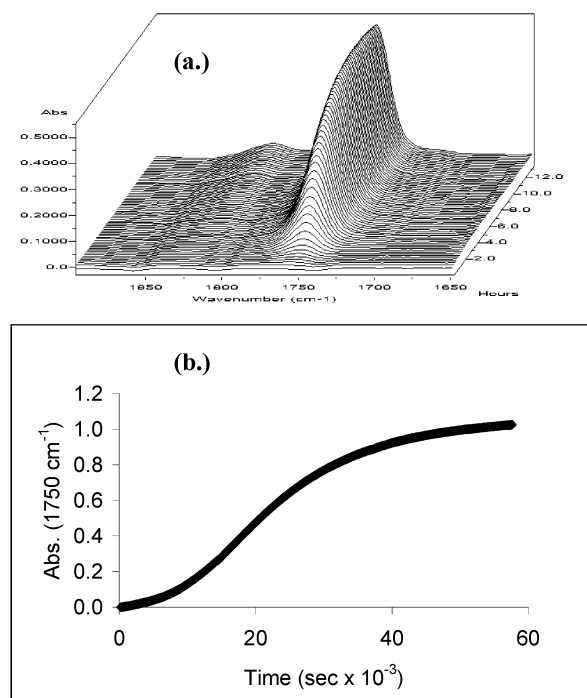


**Figure 1.** (a) Three-dimensional stack plot of the IR spectra collected every 2 min, during the reaction of CO<sub>2</sub> and propylene oxide. (b) Time profile of the absorbance at 1752 cm<sup>-1</sup> (corresponding to the poly(propylene carbonate)).

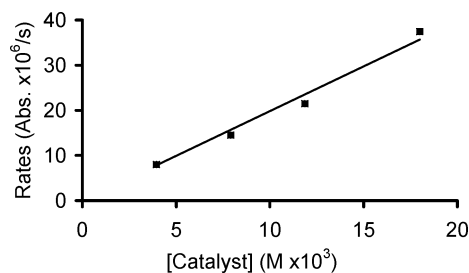


**Figure 2.** Plot of the rates of copolymerization as a function of [Cr], for the copolymerization of CO<sub>2</sub> and propylene oxide, employing complex **1** as catalyst.

of a unimolecular depolymerization reaction of the polymer–catalyst complex, i.e., a backbiting mechanism.<sup>16</sup> We have previously reported for several zinc-based catalysts that the rate of cyclic carbonate formation is much more temperature-dependent than chain propagation, with enchainment favored at lower temperatures.<sup>2f,g,17</sup> Recently, further confirmation of this has been demonstrated by Coates and co-workers for their highly active  $\beta$ -diiminate zinc initiators.<sup>18</sup> A better quantitative understanding of these two competing processes, substrate enchainment vs cyclic carbonate release, is essential to achieving full optimization of copolymer production while effectively eliminating cyclic carbonate formation.

To this end, we have conducted another series of copolymerization reactions focusing on the effect of temperature on the rates of polycarbonate vs cyclic carbonate production for both cyclohexene oxide and propylene oxide as substrates with carbon dioxide. Experimental runs were carried out employing identical

**Table 2.** Reaction Conditions and Variable-Temperature Rate Data for Copolymerization Reactions<sup>a</sup>

| temp (K) | epoxide <sup>b</sup> | rate (abs/s $\times 10^5$ ) |                  |
|----------|----------------------|-----------------------------|------------------|
|          |                      | polymer                     | cyclic carbonate |
| 303      | PO                   | 3.893                       |                  |
| 323      | PO                   | 20.72                       |                  |
| 338      | PO                   | 64.36                       | 3.213            |
| 353      | PO                   | 172.3                       | 15.51            |
| 373      | PO                   |                             | 92.74            |
| 338      | CHO                  | 0.4614                      | 0.023            |
| 348      | CHO                  | 0.7256                      | 0.11             |
| 358      | CHO                  | 1.171                       | 0.3218           |

<sup>a</sup> Each experiment was performed under 700 psi in CO<sub>2</sub>, 30 mL of the appropriate epoxide, and 50 mg of complex **1**. <sup>b</sup> PO = propylene oxide and CHO = cyclohexene oxide.

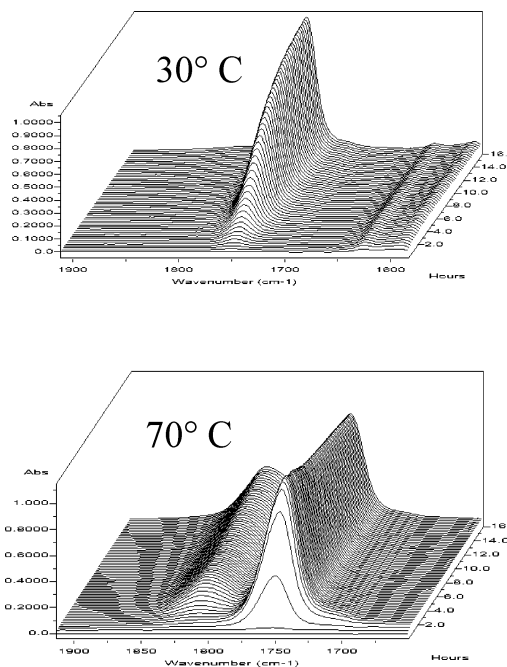


**Figure 3.** Three-dimensional stack plots of the copolymerization of CO<sub>2</sub> and propylene oxide at 30 and 70 °C.

reaction conditions in 30 mL of neat epoxide monomer with a catalyst (**1**) loading of 50 mg. Table 2 lists the initial reaction rates for production of copolymer and cyclic carbonate for both epoxide monomers as a function of temperature. Figure 3 illustrates the reaction profiles for the propylene oxide/carbon dioxide copolymerization process at two different temperatures, where at the higher temperature the copolymer is seen to degrade to propylene carbonate. The energies of activation for copolymer and cyclic carbonate formation for both cyclohexene oxide and propylene oxide were derived from these kinetic data as illustrated in Figure 4 for the latter case. Using these activation parameters, we arrived at the reaction coordinate diagrams for each process as depicted in Figures 5 and 6.

As is readily apparent from the reaction profile for the cyclohexene oxide/carbon dioxide copolymerization process, the activation barrier for cyclic carbonate formation is  $>80 \text{ kJ}\cdot\text{mol}^{-1}$  higher in energy than that of copolymer production. As previously noted, this has been *qualitatively* observed to be the case for the wide variety of zinc derived catalysts examined.<sup>2</sup> We have ascribed this to the ring strain placed on the five-membered carbonate ring in order to accommodate the conformational requirements of the alicyclic cyclohexyl ring. Obvi-

(16) Kuran, W.; Listos, T. *Macromol. Chem. Phys.* **1994**, *195*, 977–984.

(17) Darensbourg, D. J.; Wildeson, J. R.; Yarbrough, J. C. *Inorg. Chem.* **2002**, *41*, 973–980.

(18) Allen, S. D.; Moore, D. R.; Lobkovsky, E. B.; Coates, G. W. *J. Am. Chem. Soc.* **2002**, *124*, 14284–14285.

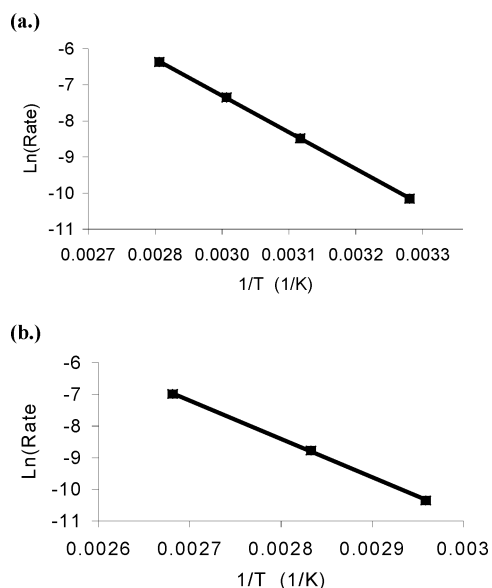


**Figure 4.** Arrhenius plots for the formation of (a) PPC (polypropylene carbonate) and (b) CPC (cyclic propylene carbonate).

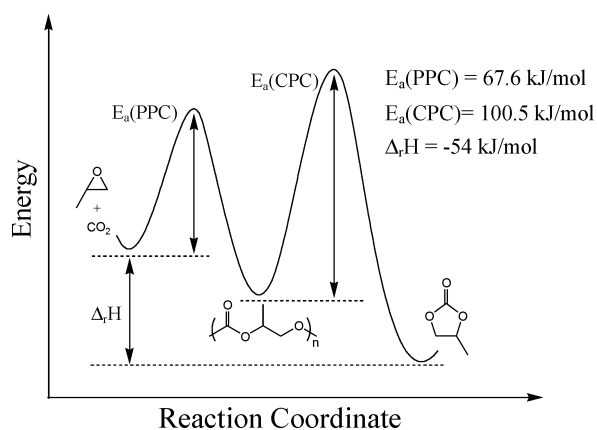


**Figure 5.** Reaction coordinate diagram for the coupling of  $\text{CO}_2$  and PO.

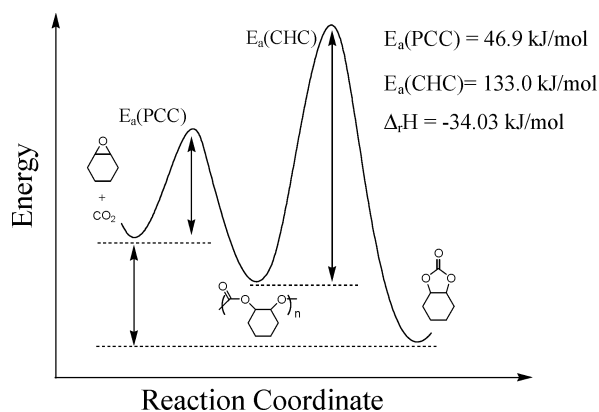


**Figure 6.** Reaction coordinate diagram of the coupling reaction of  $\text{CO}_2$  and CHO.

ously, the same is not true for the case of aliphatic epoxides such as propylene oxide. This is evident from a comparison of crystal structure data (Figure 7) of cyclic propylene carbonate and cyclic cyclohexylene carbonate.<sup>19,20</sup> Indeed, the difference

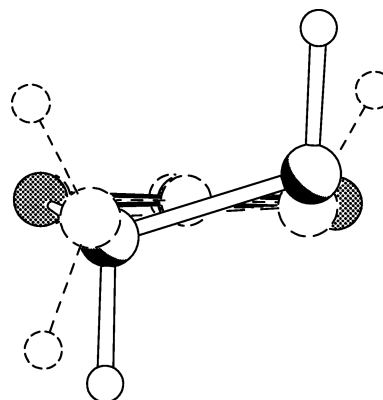


**Figure 7.** Overlay of the carbonate groups from propylene carbonate (dotted)<sup>19</sup> and cyclohexylene carbonate (solid).<sup>20</sup>

**Table 3.** Selected Bond Distances (Å) and Angles (deg) for **2b**<sup>a</sup>

|                     |           |                     |          |
|---------------------|-----------|---------------------|----------|
| Cr(1A)–O(1A)        | 1.916(7)  | Cr(1A)–O(2A)        | 1.948(6) |
| Cr(1A)–N(1A)        | 2.113(10) | Cr(1A)–N(2A)        | 2.115(9) |
| Cr(1A)–N(3A)        | 2.082(8)  | Cr(1A)–Cl(1A)       | 2.314(3) |
| O(1A)–Cr(1A)–O(2A)  | 87.9(3)   | O(2A)–Cr(1A)–N(1A)  | 91.3(3)  |
| O(2A)–Cr(1A)–N(2A)  | 90.9(3)   | O(2A)–Cr(1A)–N(3A)  | 87.3(3)  |
| O(1A)–Cr(1A)–N(2A)  | 91.1(3)   | O(1A)–Cr(1A)–N(3A)  | 88.9(3)  |
| O(1A)–Cr(1A)–N(1A)  | 178.9(3)  | N(2A)–Cr(1A)–N(3A)  | 178.2(3) |
| N(1A)–Cr(1A)–N(2A)  | 89.7(3)   | N(1A)–Cr(1A)–N(3A)  | 90.4(3)  |
| O(2A)–Cr(1A)–Cl(1A) | 177.6(2)  | O(1A)–Cr(1A)–Cl(1A) | 94.5(2)  |
| N(1A)–Cr(1A)–Cl(1A) | 86.3(2)   | N(2A)–Cr(1A)–Cl(1A) | 88.9(2)  |
| N(3A)–Cr(1A)–Cl(1A) | 92.9(3)   |                     |          |

<sup>a</sup> Estimated standard deviations are given in parentheses.

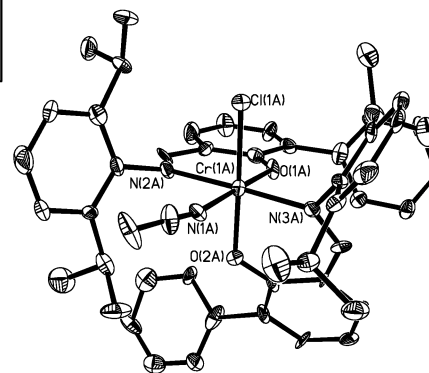
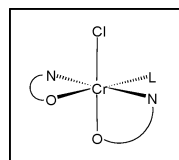


**Figure 8.** Thermal ellipsoid drawing of compound **2b** along with partial atomic numbering scheme. Inset shows stick drawing of structure.

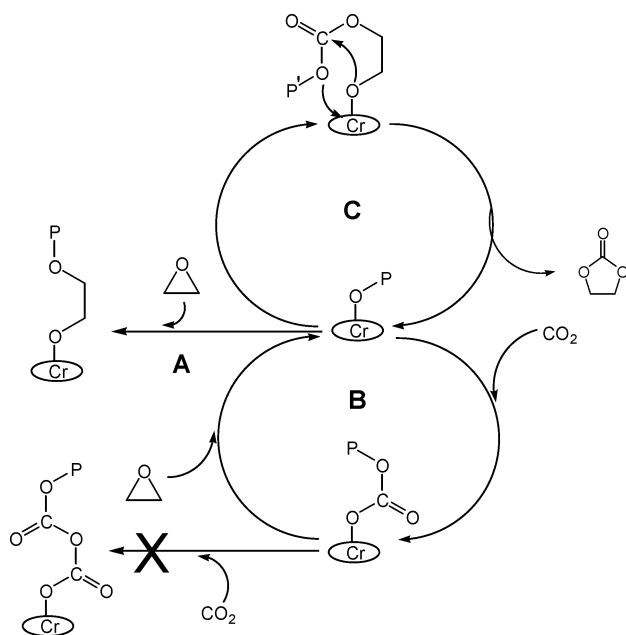
in the energies of activation for cyclic carbonate vs copolymer formation in the propylene oxide case is only  $33 \text{ kJ}\cdot\text{mol}^{-1}$ . This explains the tendency to produce large quantities of cyclic carbonate in the coupling reaction of propylene oxide and carbon dioxide for reactions carried out at elevated temperatures.

An additional point of interest concerning our proposed mechanism of copolymerization is the lack of prior coordination (or activation) of the epoxide at the metal center before ring-opening and insertion. To explore this characteristic we have designed a chromium(III) chloride complex analogous to the salen derivatives, but using two salicyaldimine ligands in place of the salen ligand. This allows for the binding of the epoxide in a site cis to the nucleophile and the growing polymer chain. The synthetic procedures for these complexes are provided in the Experimental Section. X-ray quality crystals of **2b** were

(19) Darensbourg, D. J.; Holtcamp, M. W.; Khandelwal, B.; Klausmeyer, K.; Reibenspies, J. H. *J. Am. Chem. Soc.* **1995**, *117*, 538–539.

(20) Darensbourg, D. J.; Lewis, S. J.; Rodgers, J. L.; Yarbrough, J. C. *Inorg. Chem.* **2003**, *42*, 581–589.

Scheme 2



obtained by slow diffusion of pentane into a toluene solution of the complex. Crystallographic data and data collection parameters are given in Table 1. Selected bond distances and angles are given for one of the two unique molecules in the unit cell in Table 3. Figure 8 shows a thermal ellipsoid drawing of complex **2b**, along with atomic numbering scheme. It is apparent from this drawing that the labile ligand (acetonitrile) is located at a site cis to the nucleophile (chloride ligand). Alternatively, it is possible to isolate complex **2b** without the addition of a bound acetonitrile ligand. Presumably, this five-coordinate derivative possesses a square-pyramidal geometry as reported for its ethyl analogue.<sup>10b</sup> Complex **2b** was employed as a potential catalyst for the copolymerization of cyclohexene oxide (20 mL) and carbon dioxide (700 psi) at 80 °C for a 24 h reaction period. A polymer was isolated *in low yield* with equal quantities of polyether/polycarbonate linkages along with a comparable amount of cyclic carbonate. Upon carrying out

this identical reaction in the presence of 2.25 equiv of NMeIm, a significant reduction in product yield resulted with a similar distribution of polymer/cyclic carbonate content. Hence, it can be concluded that providing a site for epoxide binding, which is inhibited in the presence of NMeIm, leads to a rather ineffective catalyst for the copolymerization process. Indeed, complex **2b** is dramatically inferior to the Cr(salen)Cl catalyst reported herein, suggesting a different catalyst structure and reaction pathway between the half-salen and salen ligand systems.

### Concluding Remarks

Scheme 2 summarizes the possible reaction modes operative during the copolymerization of carbon dioxide and epoxides utilizing Cr(salen)Cl as catalysts. Whereas pathways B and C are greatly enhanced by a more electron-rich metal center, pathway A, which affords the undesirable ether linkages, should be repressed under such circumstances. The former effect can be achieved by the substituents on the salen ligand or by addition of a donor cocatalyst such as *N*-methylimidazole. The relative importance of routes B and C is highly dependent on the nature of the epoxide. For example, pathway C is of less importance for *alicyclic* epoxides as compared to *aliphatic* epoxides. Concomitantly, in the latter instance cyclic carbonate production can be considerably suppressed by the judicious choice of reaction temperature. Current efforts are underway to examine a wide range of electronic and steric variations of the salen ligand, as well as the role of the cocatalyst on the kinetic parameters of the carbon dioxide/epoxide copolymerization process to further address these issues.

**Acknowledgment.** Financial support from the National Science Foundation (Grants CHE 99-10342 and CHE 02-34860), from NSF Grant CHE 98-07975 for the purchase of X-ray equipment, and from the Robert A. Welch Foundation is greatly appreciated.

**Supporting Information Available:** Complete details of the X-ray diffraction study of complex **2b** (PDF). This material is available free of charge via the Internet at <http://pubs.acs.org>.

JA034863E